Journal of Environment and Engineering

Vol. 5, No. 1, 2010

# Detection of Cavitation with Accelerometers Mounted on Piping Outer Surfaces*

Shigeo MIZUYAMA**, Michio MURASE***, Yuzo FUJII****
and Yoshinori YAGI*****

** Institute of Nuclear Safety System, Inc., Present address: The Kansai Electric Power Co., Ltd.
1-1Yosimi, Ohshima-1, Ohi-cho, Ohi-gun, Fukui 919-2101, Japan
*** Institute of Nuclear Safety System, Inc.
64 Sata, Mihama-cho, Mikata-gun, Fukui 919-1205, Japan
E-mail: murase@inss.co.jp
**** Institute of Nuclear Safety System, Inc., Present address: Japan NUS Co., Ltd.
9-15 Kaigan 3-chome, Minato-ku, Tokyo 108-0022, Japan
***** Institute of Nuclear Safety System, Inc., Present address: The Kansai Electric Power Co., Ltd.
Tanoura, Takahama-cho, Ohi-gun, Fukui 919-2392, Japan

**Abstract**

Cavitation-induced vibration and erosion of pipes is a potentially damaging factor in piping systems. To prevent it, a detection method for cavitation phenomena should be developed. In power plants, especially, it is desirable to detect them from outside pipes during operation. Detection of cavitation phenomena was experimentally investigated in this paper using accelerometers mounted on the outer surface of a pipe upstream and downstream from an orifice. The following results were obtained. (1) With the progression of cavitation, output voltage of the accelerometer varied, and the amplitude and number of the pulse-shaped signals increased. However, it would likely be difficult to distinguish them from noises in an operating plant. (2) It was difficult to recognize the characteristic frequency of cavitation, because the power spectrum density was broad up to the accelerometer limit of 45 kHz. (3) The flow directional distribution of RMS (root mean square) values of accelerometer output voltage varied greatly with the progression of cavitation. Therefore, from comparison of RMS values obtained upstream and downstream from the orifice it seems possible to detect cavitation phenomena in the piping systems of operating plants.

***Key words***: Cavitation, Power Plant, Pipeline Component, Orifice, Accelerometer, Detection

## 1. Introduction

A local increase in flow velocity in a valve or orifice, where the flow area decreases, causes the fluid pressure to drop, and cavitation bubbles appear when the pressure falls below the saturated vapor pressure. With the decrease of flow velocity downstream from the throttle, the fluid pressure rise causes the cavitation bubbles to collapse and impact pressures occur due to the bubble collapse. The impact pressures bring about erosion of the pipe wall and vibration of the piping systems, which are potentially responsible for damage to those systems[1-2]. Piping systems are designed to avoid cavitation during normal operation. During transient operation at the plant startup and shutdown, however, there is a potential for cavitation occurrence, and coolant leakage has occurred due to a crack at a pipe welding caused by cavitation-induced vibration[3]. Therefore, a cavitation detection

*Received 25 Aug., 2009 (No. T1-07-7040)
Japanese Original : Trans. Jpn. Soc. Mech. Eng., Vol.74, No.743, C (2008), pp.1681-1687 (Received 12 Dec., 2007)
[DOI: 10.1299/jee.5.200]

method which can be used during plant operation should be developed in order to prevent such problems.

Regarding pump cavitation, the Turbomachinery Society of Japan has published the *Guideline for Prediction and Evaluation of Cavitation Erosion in Pumps*[4] which describes methods to detect and evaluate cavitation using accelerometers, AE (acoustic emission) sensors and underwater microphones. Sawada et al.[5] conducted experiments to detect cavitation in a waterwheel using acoustic emission. In a plant piping system, however, there are many elements such as valves and orifices other than pumps, where cavitation may occur, and devices to measure pressure and flow rate are not equipped on most of them. Therefore, it is difficult to evaluate cavitation number at those elements and prepare a data base for judgment of cavitation occurrence in advance. No studies on cavitation detection at valves and orifices in an operating plant have been reported.

The objective of this study is to develop a detection method of cavitation phenomena at the valves and orifices in plant piping systems without preparing a data base for judgment of cavitation occurrence. We focus on cavitation downstream from a throttle such as a valve and an orifice and its effects on a pipe wall, which is the pressure boundary. In plants, it is desirable to use microphones which do not touch the pipes. As an essential first step to apply microphones, however, we used accelerometers in this paper in order to evaluate the relationship between the behavior in a pipe and detection characteristics on its outer surface. We carried out visualizations of the cavitation field downstream from an orifice, measurements of erosion distribution on the inner surface and measurements using accelerometers mounted on the outer surface of the pipe, and evaluated the possibility for cavitation detection in an operating plant piping system.

## 2. Experimental Apparatus and Method

### 2.1 Test apparatus and test section

Figure 1 shows the closed test loop which consists of a reservoir, pump, test section and pipe system. The reservoir is a pressure vessel (volume, 1.28 $m^3$) and the pressure at the safety relief valve is 3.2 MPa. Water temperature can be raised to 150 ℃ by electric heaters installed in the reservoir. The flow rate is measured by an electromagnetic flow meter upstream from the test section and pressures are measured both upstream and downstream from the test section. Water temperature is measured by a thermocouple in the reservoir. The pressure in the test section is controlled by the nitrogen tank connected with the reservoir. The flow rate and velocity in the test section are adjusted by inverter control of the pump. Ordinary tap water is used as working fluid. Dissolved oxygen concentration is measured before and after tests, because the concentration of dissolved gas in the working fluid may affect bubble occurrence and impact pressures due to bubble collapse.

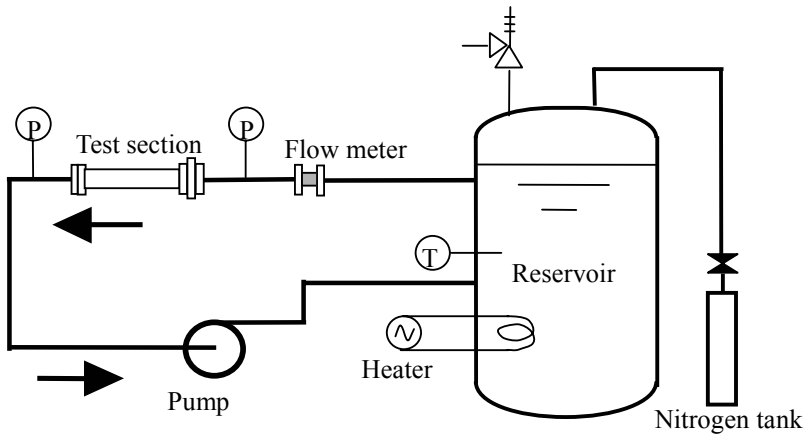


Fig. 1 Test loop

Figure 2 shows the test section, which consists of a pipe and an orifice. The pipe (inner diameter, 49.5 mm) is made of acrylic resin or stainless steel, SUS 304. The orifice has a length of 28 mm and diameter of 24.75 mm, and it is made of stainless steel, SUS 304.

We used the acrylic resin test section for observation of the cavitation field and measurements of cavitation erosion, where erosion test specimens (Fig. 3) were inserted in the pipe wall. The erosion test specimens were made of pure copper, C1100BD-H, in order to decrease the effects of unevenness due to erosion on the flow field and to shorten the erosion time.

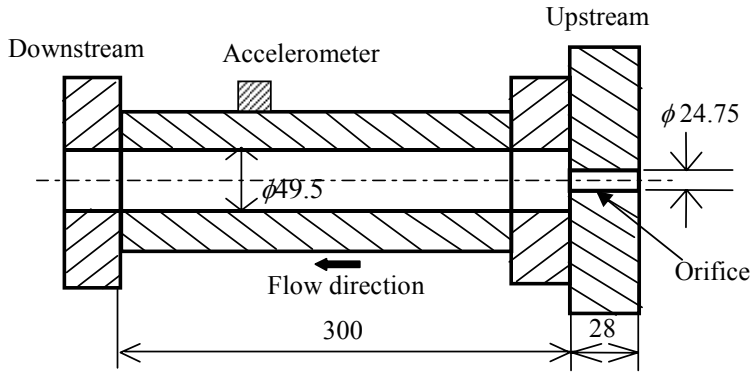


Fig. 2 Test section (unit: mm)

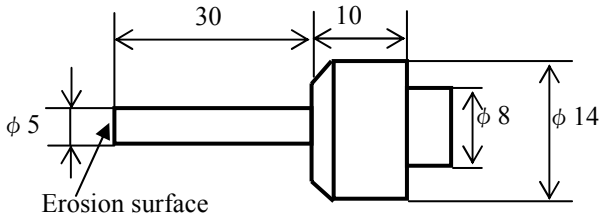


Fig. 3 Erosion test specimen (unit: mm)

**2.2 Test conditions**

Cavitation number was used for the test parameter and it is defined by:

$$\sigma = \frac{2(P - P_v)}{\rho V_o^2}$$

where $P$ [Pa] is the pressure downstream from the orifice, $P_v$ [Pa] is the saturated vapor pressure, $V_o$ [m/s] is the average velocity in the orifice and $\rho$ [kg/m3] is the water density.

The tests in this study were conducted at a water temperature of 24-27 ℃ and constant flow velocity of $V_o$ = 15.0-15.4 m/s. The cavitation number was adjusted by controlling the pressure in the reservoir and the pressure downstream from the orifice, $P$. The effects of setting errors and fluctuations of $V_o$ and $P$ on the cavitation number were within $\pm 0.03$. The dissolved oxygen concentration during the tests was 3.77-6.55 g/m$^3$.

**2.3 Measurements by accelerometer**

It has been reported that the predominant frequency is several decades of kHz[6] when acceleration on the acrylic pipe wall caused by bubble collapse is measured using an accelerometer. Additionally, it has been reported that the high frequency region over 10 kHz is important[7] when the erosion rate is predicted from outputs of sensors. Therefore, in this study, we used piezo-electric accelerometers with a high frequency range (TEAC, 703FB, 0.3-45 kHz ±3 dB). Figure 4 shows the measurement system using accelerometers. Each

accelerometer was mounted on the outer surface of the test section using double-sided sticky tape and then fixed using a resin band. Output voltage of each accelerometer was stored in a digital oscilloscope through an amplifier, and treatment of the measured values was done using a personal computer.

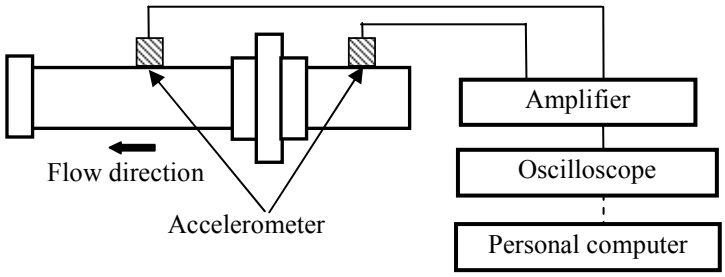


Fig. 4 Measurement system

## 3. Measured Results and Discussion

### 3.1 Output characteristics of accelerometer

Figure 5 shows observations of the cavitation field and output voltage of one accelerometer at the cavitation numbers of $\sigma = 2.8$, 1.4 and 0.7 for the stages of no cavitation bubbles, initial cavitation and developed cavitation, respectively, which were determined from cavitation bubbles observed downstream from the orifice. In the measurements, the test section made of stainless steel was used and the measurements were made 100 mm downstream from the orifice outlet, where cavitation bubbles were near the pipe inner surface in the case of developed cavitation. At $\sigma = 2.8$, the output voltage was very small comparing with that under cavitation conditions. At $\sigma = 1.4$ in the stage of initial cavitation, the output voltage was small, but pulse-shaped signals were detected. At $\sigma = 0.7$ in the stage of developed cavitation, pulse-shaped signals with large output voltage were detected and their frequency increased. It seems that the accelerometer detected impact pressures caused by collapse of cavitation bubbles as pulse-shaped signals. Therefore, in the stage of developed cavitation like $\sigma = 0.7$, it may be possible to detect the cavitation phenomena from the detection of pulse-shaped signals and to evaluate the strength of cavitation from the amplitude and frequency of these pulse-shaped signals. In an operating plant, however, the situation differs from that within a test facility, and various kinds of noise caused by pumps and motors may be detected. Thus, it may be difficult to judge the detected pulse-shaped signals as pulses caused by cavitation.

In order to evaluate the effects of the cavitation number on acceleration, we measured acceleration on the pipe wall at 75 mm downstream from the orifice, while changing the cavitation number. The velocity was constant at $V_o = 15$ m/s. Accelerometer output voltage at 75 mm downstream from the orifice is shown in Fig. 6. The vertical axis shows the average of 5 output voltage RMS (root mean square) values normalized by the average of 5 output voltage RMS values at $\sigma = 2.8$ without cavitation, which was about 0.47 mV. At about $\sigma = 2.6$, the RMS value started to increase, and cavitation bubbles were very small and difficult to see. The RMS value increased until about $\sigma = 2.0$, then decreased for $\sigma < 2.0$, and had a local minimum at about $\sigma = 1.4$. At about $\sigma = 1.6$, cavitation bubbles could be clearly observed. Therefore, we defined the stage of initial cavitation as in the region of $\sigma > 1.4$. However, it should be noted that the RMS value was relatively large in the region of $1.8 \le \sigma \le 2.4$ due to cavitation inside the orifice. As for decreasing the cavitation number from $\sigma = 1.4$, the RMS value increased and became the maximum at about $\sigma = 0.6$. In the region of $\sigma < 0.6$, the RMS value decreased and super cavitation occurred at about $\sigma = 0.4$.

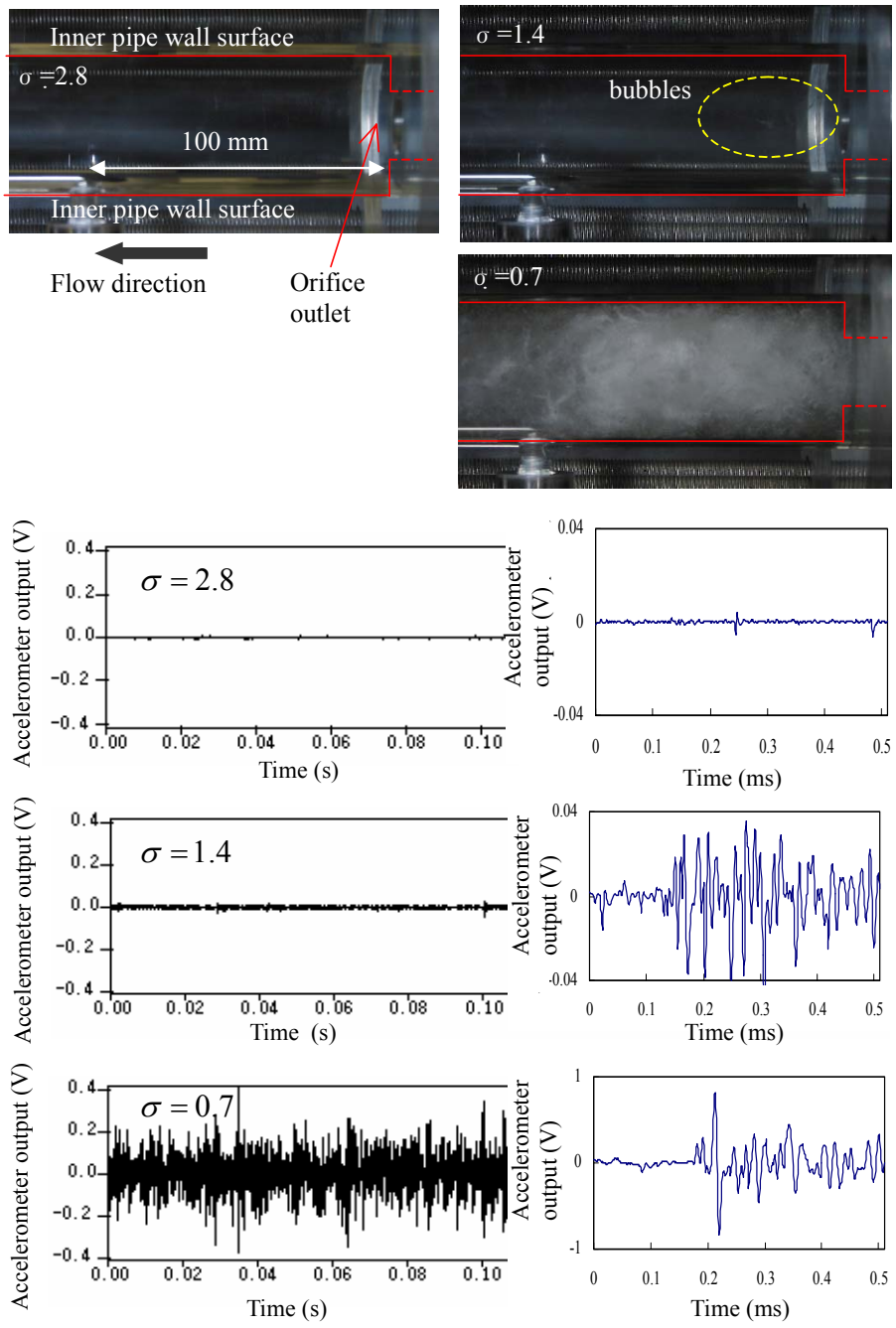


Fig. 5 Flow conditions and output voltage at 100 mm downstream from orifice

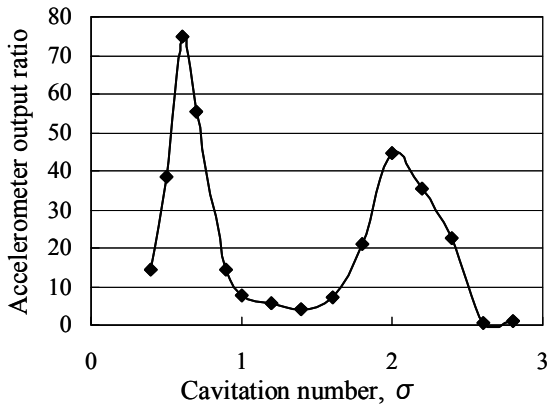


Fig. 6 Accelerometer output RMS ratio at 75 mm downstream from orifice

### 3.2 Frequency analysis

If there is a characteristic frequency in the accelerometer output voltage caused by collapse of cavitation bubbles, we can separate it from noises in an operating plant and detect cavitation. Therefore, we conducted frequency analyses for output voltage of the accelerometer mounted on the outer surface of the acrylic pipe or stainless steel pipe at 100 mm downstream from the orifice. Figure 7 shows the results of frequency analyses using a low-pass filter of 500 kHz to cut the effects of noise from the inverter for the flow rate control of the pump.

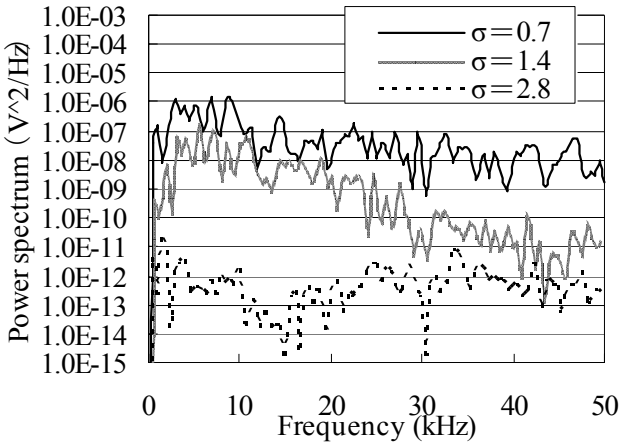


(a) Acrylic pipe

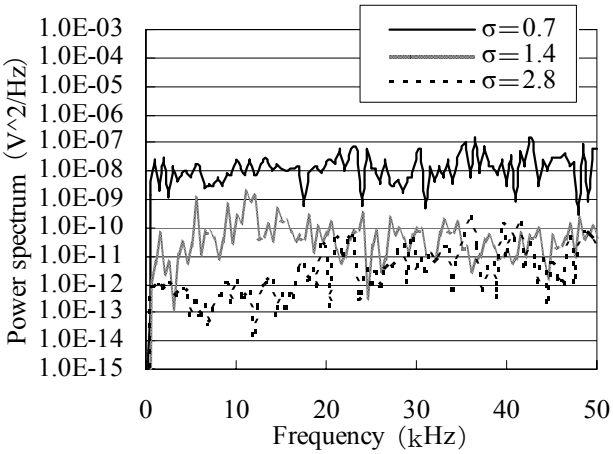


(b) Stainless steel pipe

Fig. 7 Frequency analysis of accelerometer output voltage at 100 mm downstream from orifice

In the tests using the acrylic pipe, compared with the power spectrum at $\sigma = 2.8$ without cavitation, the power spectrum in the stage of initial cavitation at $\sigma = 1.4$ increased in the region below 30 kHz and the power spectrum lower than 10 kHz was several orders larger than the high-frequency components over 30 kHz. In the stage of developed cavitation at $\sigma = 0.7$, the power spectrum increased in the whole frequency range and the power spectrum lower than 10 kHz was one order larger than the high-frequency components over 10 kHz. On the other hand, in the tests using the stainless steel pipe, the power spectrum increased in the region below 20 kHz at $\sigma = 1.4$ compared with the power spectrum at $\sigma = 2.8$ and the power spectrum at about 10 kHz was one order larger than the frequency components over 20 kHz. In the stage of developed cavitation at $\sigma = 0.7$, however, the power spectrum increased in the whole frequency

range and many peaks appeared over 20 kHz.

The results shown in Fig. 7 indicate that the power spectrum measured by the accelerometer depends on the pipe material and that high-frequency components are larger in the stainless steel pipe than in the acrylic pipe, which means that decay in the acrylic resin is large especially in the high-frequency region. Moreover, even in the same-material pipe, frequency characteristics of the accelerometer output voltage depend on the cavitation number. Therefore, it may be difficult to judge occurrence and strength of cavitation from the frequency analyses of the accelerometer output voltage. In order to do so, a sufficiently large enough data base for the objects of cavitation detection such as valves and orifices is required.

**3.3 Flow directional distribution of output voltage**

Cavitation bubbles generally appear downstream from a throttle and it is expected that the accelerometer output voltage is larger downstream than upstream. On the other hand, the effects of vibration and noise from other sources on the accelerometer output voltage may be similar both upstream and downstream. Therefore, we measured flow directional distributions of the accelerometer output voltage, and evaluated the possibility of cavitation detection. We conducted tests at $\sigma = 2.8$, 1.4 and 0.7, and made measurements at 300 mm and 90 mm upstream from the orifice, and 50 mm, 75 mm, 100 mm, 170 mm and 270 mm downstream from it. For $\sigma = 0.7$, the accelerometer output voltage was additionally measured at 35 mm downstream from the orifice. Figure 8 shows flow directional distributions for RMS values of the accelerometer output voltage. In case (a) at $\sigma = 2.8$, the maximum RMS value was very small at 0.47 mV and there were no clear differences between RMS values upstream and downstream from the orifice. The results show that there were no impact pressures caused by collapse of cavitation bubbles. In case (b) at $\sigma = 1.4$, the maximum RMS value was 5.5 mV, which was over 10 times larger than that at $\sigma = 2.8$. The RMS values upstream from the orifice were larger than those downstream from it and their ratio was about 2. In this case, collapse of cavitation bubbles occurred in the orifice near the inlet and it seems that impact pressures might mainly propagate upstream. In case (c) at $\sigma = 0.7$, the maximum RMS value was 74.9 mV, which was over 10 times larger than that at $\sigma = 1.4$. The maximum RMS value downstream was over 10 times larger than the RMS value upstream, the results showed that collapse of cavitation bubbles caused a large impact pressure on the pipe wall in the downstream region. As shown in Fig. 8, from the flow directional distribution of the accelerometer output voltage, it is possible to detect locations where impact pressures act.

In order to confirm the relationship between the location where an impact pressure was acting and accelerometer output voltage, we measured the flow directional distribution of erosion. In the erosion measurements, the erosion test specimen surface (Fig. 3) was mirror finished, and each erosion test specimen was inserted into the pipe wall and adjusted so that there would be no unevenness between the specimen surface and the wall inner surface. The weight of the erosion test specimen was measured before and after tests using a precision balance with the minimum indication of 0.01 mg, and the erosion rate was obtained from the change of weight and test time. Because the erosion rate depends on the test time, we used the erosion rate when it had reached the maximum and was almost constant. Figure 9 shows the flow directional distribution of erosion rates at the cavitation number of 0.7. In the figure, the average, maximum and minimum values of erosion rates among five measurements are shown. The peak location of erosion rates was in the region of 60-75 mm from the orifice outlet, which agreed with the peak location of RMS values being at about 75 mm as shown in Fig. 8 (c).

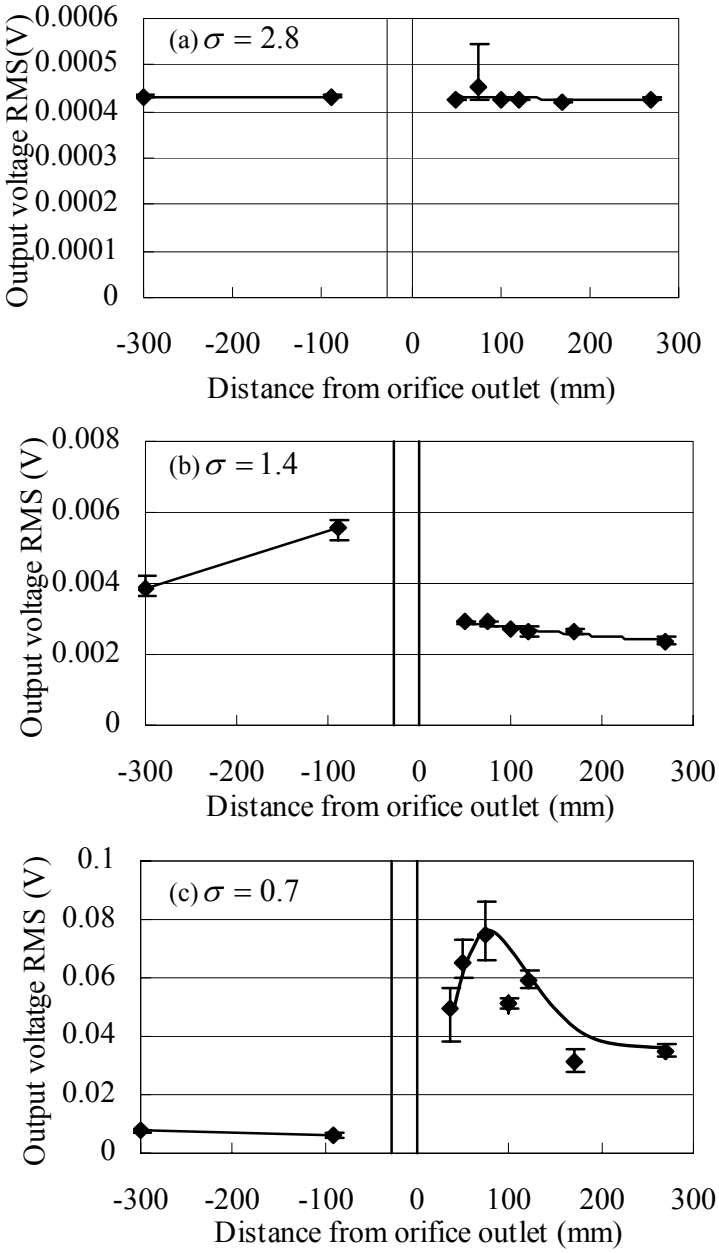


Fig. 8 Flow directional distribution for RMS values of accelerometer output voltage at different cavitation numbers

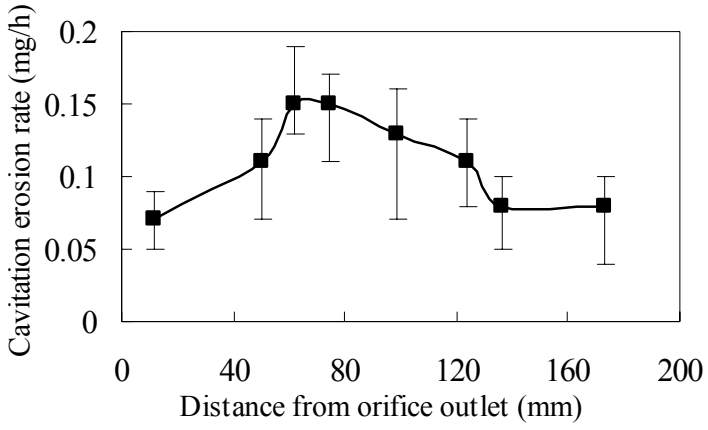


Fig. 9 Distribution of cavitation erosion rate at $\sigma = 0.7$

### 3.4 Ratio of output voltage upstream and downstream from the orifice

We conducted simultaneous measurements using two accelerometers mounted at 90 mm upstream and 75 mm downstream from the orifice outlet, where the erosion rate was the maximum. Figure 10 compares RMS values of the accelerometer output voltage upstream and downstream from the orifice. Figure 11 shows the RMS ratio of the accelerometer output voltage downstream and upstream from the orifice. Because gain of each accelerometer is different, RMS ratios were normalized in the figure using the RMS ratio at $\sigma = 2.8$. Measurements were conducted five times, and the average, maximum and minimum values are shown.

With decreasing cavitation number, the RMS value upstream increased after cavitation occurrence, and became the maximum at about $\sigma = 1.6$. The RMS value upstream was larger than the RMS value downstream in the region of $1.4 \le \sigma \le 1.8$, but did not increase in the stage of developed cavitation and its dispersion was small. On the other hand, the RMS value downstream was larger than the RMS value upstream in the stage of developed cavitation for $\sigma \le 0.9$ and its dispersion was large. From the results shown in Fig. 11, we judged there was transition of cavitation when the RMS ratio between downstream and upstream values was larger than 4.0 and its dispersion was large. However, even when the RMS ratio was lower than 4.0, cavitation occurred. As for the stage of initial cavitation in the region of $1.6 \le \sigma \le 2.4$, the RMS value was relatively large as shown in Fig. 10 due to cavitation in the orifice and its classification method is an issue that remains for further investigation.

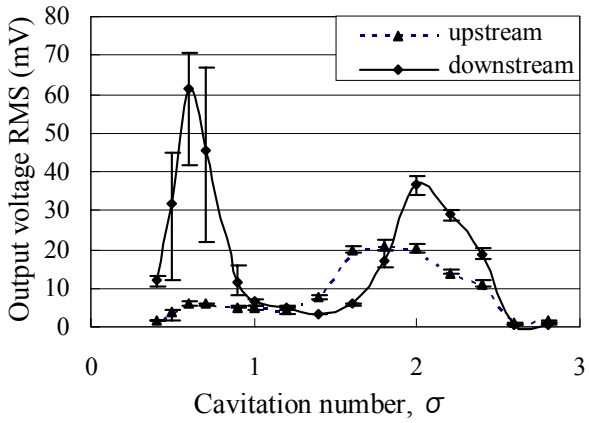


Fig. 10 RMS values of accelerometer output voltage at upstream and downstream of orifice

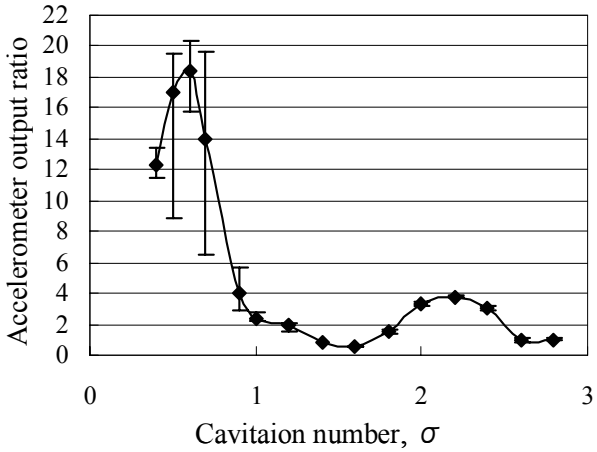


Fig. 11 RMS ratio of accelerometer output voltage between downstream and upstream

### 3.5 Discussion

Cavitation measurements have been conducted using an accelerometer, AE sensor and microphone, and it is well known that output signals change due to the cavitation number. However, in order to detect cavitation in an operating plant without a data base on output characteristics caused by cavitation, quantitative change is not detected, but rather qualitative change.

We evaluated frequency characteristics of accelerometer output voltage. In the stainless steel pipe, however, there were many peaks in the power spectrum up to the accelerometer upper limit of 45 kHz as shown in Fig. 7 (b) and we could not specify a characteristic frequency for cavitation. On the other hand, when we conducted frequency analysis only for the pulse-shape signal like that shown in Fig. A in the Appendix, a clear peak of frequency was obtained at 20-25 kHz in the acrylic pipe and at 35-50 kHz in the stainless steel pipe. This means that decay of high-frequency signals is large in the acrylic pipe.

The flow directional distribution of the RMS values of the accelerometer output voltage was similar to the flow directional distribution of erosion (compare Fig. 8 (c) with Fig. 9). Applying the results, we can detect the occurrence of the stage of developed cavitation from the RMS ratio of the accelerometer output voltage upstream and downstream from a throttle in an operating plant without the data base to judge cavitation states (see Figs. 10 and 11). Moreover, from the simultaneous measurements with plural accelerometers mounted at different flow directional locations, we can evaluate the location where an impact pressure acts and confirm that the pulse-shaped signal is caused by the impact pressure due to collapse of cavitation bubbles. An example is shown in the Appendix.

There are some remaining technical issues. As shown in Figs. 10 and 11, the RMS ratio of the accelerometer output voltage upstream and downstream from the orifice is almost the same at about $\sigma = 1.4$. Therefore, when the RMS value of the accelerometer output voltage is large and there is a possibility of cavitation occurrence, detailed measurements of the flow directional distribution of the accelerometer output voltage like Fig. 8 (b) are required. The important issue of this study is to confirm the effectiveness of the proposed cavitation detection method in Fig.11 in order to prevent cavitation erosion, namely to evaluate the relationship between the cavitation detectable region and cavitation erosion conditions. Additionally, accelerometers have demerits that their setting time is long and objects where measurements can be made are limited to low temperature pipes. Therefore, it is more desirable to use microphones, which are easy to use in a plant, even though signals from impact pressures become weak.

## 4. Conclusions

We conducted tests to detect cavitation phenomena using accelerometers mounted on the outer surface of a pipe with an orifice, and obtained the following results.

(1) As cavitation develops (i.e. decreasing the cavitation number), the number of pulse-shaped signals in the accelerometer output voltage increased and the amplitude of the pulse-shaped signals increased. In order to use this information for cavitation detection in an operating plant, however, it should be confirmed that these pulse-shaped signals are not noise but signals from impact pressures caused by collapse of cavitation bubbles, and a data base to compare amplitudes of the pulse-shaped signals is needed.

(2) The characteristic frequency for cavitation could not be specified, because the power spectrum of the accelerometer output voltage greatly depended on the pipe material and there were many peaks in power spectrum up to the accelerometer upper limit of 45 kHz especially in the stainless steel pipe.

(3) The RMS ratio of the accelerometer output voltage upstream and downstream from the

orifice changed according to cavitation states, the RMS value upstream was about 2 times larger than the RMS value downstream in the stage of initial cavitation, and the RMS value downstream became about 10 times larger than the RMS value upstream in the stage of developed cavitation. Therefore, cavitation occurrence can be detected from the flow directional distribution of the accelerometer output voltage, which was qualitatively similar to the flow directional distribution of erosion.

Regarding use of the RMS ratio of the accelerometer output voltage upstream and downstream from the orifice mentioned in (3), measurements are needed at plural locations, but a data base to judge cavitation stages is not required and the RMS ratio can be applied to detect cavitation phenomena in an operating plant. Moreover, from the simultaneous measurements with plural accelerometers mounted at different flow directional locations, the location of an impact pressure can be identified and it can be confirmed that the pulse-shaped signals in the accelerometer output voltage are caused by the impact pressures due to collapse of cavitation bubbles.

## Acknowledgements

For construction of the test loop shown in Fig. 1 and selection of accelerometers, we referred to the test loop at the laboratory of Professor Keiichi Sato, Kanazawa Institute of Technology and experiments which his laboratory carried out. In order to shorten the test period of erosion, erosion test specimens shown in Fig. 3 were pretreated using a magnetostrictive vibrator in the laboratory of Professor Shuji Hattori, University of Fukui. We greatly appreciate their technical support.

## References

(1) J. Ozol, J. H. Kim and J. Healzer, Cavitation Experience with Control Valves in Nuclear Power Plants, *Cavitation and Gas-Liquid Flow in Fluid Machinery and Devices*, ASME, Vol. 190 (1994), pp. 291-297.

(2) P. Moussou, S. Cambier, D. Lachene, et al., Vibration Investigation of a French PWR Power Plant Piping System Caused by Cavitating Butterfly Valves, *Proceedings of Symposium on Flow-Induced Vibration*, ASME Pressure Vessels and Piping Conference, Vol. 420-2 (2001), pp. 99-109.

(3) Ministry of Economy, Trade and Industry, Nuclear and Industrial Safety Agency, Nuclear Safety Administration Division ed., *Publication of the annual report of nuclear plant operating administration* (2001), pp. 391-396, Thermal and Nuclear Power Engineering Society. (in Japanese)

(4) Turbomachinery Society of Japan ed., *Guideline for Prediction and Evaluation of Cavitation Erosion in Pumps* (2003), pp. 112-113, Turbomachinery Society of Japan. (in Japanese)

(5) A. Sawada, et al., Detection of the water wheel cavitation using acoustic emission sensor and wavelet transform, *Proceedings of the 11th Symposium on Cavitation* (2001), pp. 157-160. (in Japanese)

(6) K. Sato, Comparison of Cavitaion Shock Pressures Based on Difference of Bubble Patterns, *Transactions of the Japan Society of Mechanical Engineers, Series B*, Vol. 56, No. 532 (1990), pp. 3597-3602. (in Japanese)

(7) H. Kato, ed, *Cavitation* (1999), pp.239-240, Maki-shoten, Tokyo. (in Japanese)

## Appendix

In order to confirm that the pulse-shaped signals are caused by impact pressures due to collapse of cavitation bubbles, we conducted simultaneous measurements using three accelerometers mounted at different flow directional locations. The axis in the flow direction from the orifice outlet is $x$ and the axis in the circumferential direction from the top of the outer surface of the pipe is $y$. The locations of the three accelerometers are $S_1$ ($a$, 0), $S_2$ ($b$, 0) and $S_3$ ($c$, 0). The location of the impact pressure is ($x$, $y$), and the time is $t_i$ when the impact pressure reaches each accelerometer $S_i$ ($i$ =1, 2, 3). Then we have the following equations for the relationship between the location of each accelerometer and the propagation time of the impact pressure.

$$V_s \cdot t_1 = \sqrt{(x-a)^2 + y^2}\ ,\quad V_s(t_1 + dt_2) = \sqrt{(x-b)^2 + y^2}\ ,\quad V_s(t_1 + dt_3) = \sqrt{(x-c)^2 + y^2}\ ,$$

$$dt_j = t_j - t_1 \quad (j = 2, 3)$$

In the equations, $V_s$ [m/s] is the propagation velocity of the impact pressure in the pipe wall, flow directional locations of accelerometers, $a$, $b$ and $c$, are known, time differences of $dt_2$ and $dt_3$ are measured, and the unknown parameters are $x$, $y$ and $t_1$. In the evaluation of $x$ and $y$, we assumed the following. (1) Collapse of cavitation bubbles occurs near the inner surface of the pipe and the impact pressure acts on the inner surface of the pipe. (2) We neglect the pipe wall thickness and the impact pressure propagates in concentric circles to reach the accelerometers. (3) Sound velocity of side waves in stainless steel is 3,000 m/s.

Figure A shows output voltage of simultaneous measurements with three accelerometers, where $a$, $b$ and $c$ are 50 mm, 75 mm and 150 mm, respectively. The cavitation number is $\sigma = 0.7$. Clear time correlations between waveforms of the output voltage could not be obtained, because waveforms warped during propagation at the pipe wall. Therefore, we evaluated the location of the impact pressure using the time differences of the first peaks of the waveforms shown in Fig. A. As the result, the location of the impact pressure was $x$ =97 mm and $y$ =55 mm. The flow directional location of $x$ =97 mm is within the region of high RMS values and large erosion rates as shown in Figs. 8 (c) and 9. And the circumferential location of $y$ =55 mm (angle $\theta = 104°$ from the top) is less than $\pi R_O = 95$ mm. Therefore, the pulse-shaped signals may not be noise but may be caused by impact pressures due to collapse of cavitation bubbles.

We also conducted simultaneous measurements using two accelerometers, where a steel ball of 0.26 g was dropped between the two accelerometers. From the similarity of the waveforms of the output voltage, we confirmed that the waveforms shown in Fig. A were caused by impact pressures.

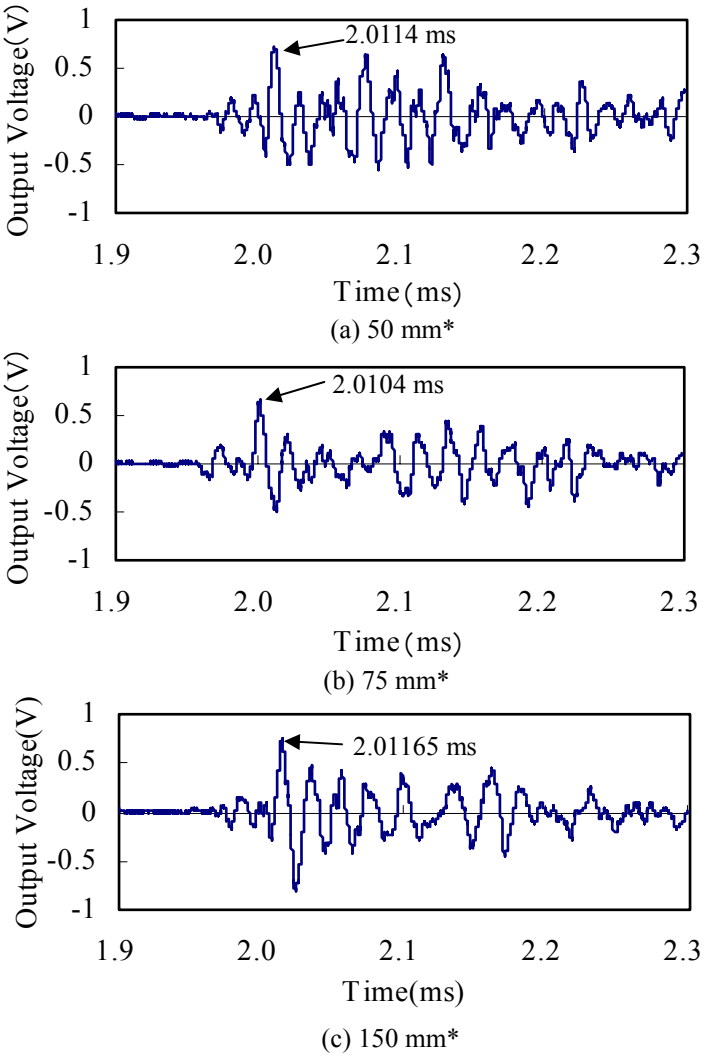


Fig. A Output voltage of simultaneous measurements with three accelerometers at $\sigma = 0.7$ (*distance from orifice outlet)